Solutions to remove a boundary image sticking in an ac plasma display panel

Choon-Sang Park and Heung-Sik Tae*

School of Electrical Engineering and Computer Science, Kyungpook National University, Daegu 702-701, South Korea

*Corresponding author: hstae@ee.knu.ac.kr

Received 26 March 2009; revised 15 June 2009; accepted 30 June 2009; posted 1 July 2009 (Doc. ID 109062); published 13 July 2009

When displaying a square-type image with peak luminance for approximately 500 h in a 42 in. plasma display panel TV with high Xe (15%) content, halo-type boundary image sticking was observed in the nondischarge region adjacent to the discharge region. The halo-type boundary image sticking phenomenon is due mainly to the redeposit of the Mg species on the MgO layer in the nondischarge region adjacent to the discharge region, which is verified by measuring the redeposited Mg species in the boundary image sticking region using a cross-sectional scanning electron microscope. Based on this result, three kinds of solution to remove the boundary image sticking of an ac plasma display panel are introduced. First, we completely recover the boundary image sticking cells by using a full-white aging process. Second, we prohibit the inherent production of boundary image sticking by sealing the plasma display panel under vacuum. The final solution is to prohibit the inherent production of boundary image sticking by use of lower gas pressure. © 2009 Optical Society of America

OCIS codes: 000.2190, 040.1520, 310.3840, 310.6845, 350.5400.

1. Introduction

The realization of a high quality plasma display panel (PDP) requires an urgent solution to image sticking or image retention problems induced in the PDP cells when strong discharges are produced repeatedly for a sustained period of time [1–13]. Image retention means a temporal image sticking that is easily recoverable with a minor procedure, whereas image sticking means a permanent sticking that is not recoverable even by use of extensive procedures. Image sticking is known to be induced even in nondischarged cells adjacent to discharged cells, which is called halo-type boundary image sticking. Our previous experimental results showed that the main culprit for inducing permanent image sticking was deeply related to the Mg species sputtered from the MgO surfaces of the discharge cells that are due to severe ion bombardment during a sustained discharge simply by monitoring the morphology change of the MgO surface and V_t closed curve analysis [6]. The deposition of the sputtered Mg species on the phosphor layer in the discharge cells, or the redeposition of the sputtered Mg species on another MgO surface of the nondischarge cells adjacent to the discharge cells, can alter the reset or sustained discharge characteristics, thus causing image sticking or boundary image sticking [6]. However, in the pervious results, the redeposition of the sputtered Mg species on another MgO surface of the nondischarge cells adjacent to the discharge cells was not verified. In addition, in the previous experiments, the discharge characteristics in the boundary image sticking region related to the redeposition phenomenon was not investigated in detail, even though two kinds of solution to remove the boundary image sticking, such as a full-white aging discharge [7] and a vacuum sealing process [8], were discussed.

Accordingly, to verify that the halo-type boundary image sticking phenomenon was due mainly to the redeposition of the Mg species on the MgO layer in the nondischarge region adjacent to the discharge region, we measured the redeposited layer on the MgO

0003-6935/09/250F76-06$15.00/0

surface in the boundary image sticking region by cross-sectional scanning electron microscope (SEM) analysis. We also investigated various methods to remove boundary image sticking in ac PDPs based on monitoring discharge characteristics.

First, the full-white aging discharge was examined to recover the boundary image sticking. Second, the vacuum sealing method was proposed to prohibit the boundary image sticking. Finally, the effects of the lower gas pressure on the production of the boundary image sticking were examined. The infrared (IR) (828 nm) emission and intensified charge-coupled device (ICCD) image of a nondischarge region adjacent to the discharge region were observed in comparison with those of a nondischarge region far from the discharge region under full-white background in a 42 in. ac PDP module. In addition, to monitor the changes in the MgO surface, a SEM was used.

2. Experimental Setup

Figure 1 shows the optical measurement systems and commercial 42 in. ac PDP module with the three electrodes that were used in the experiment, where X is the sustained electrode, Y is the scan electrode, and Z is the address electrode. A color analyzer (CA-100 Plus), an image colorimeter (Prometric PM Series camera with RGB filters), a pattern generator, a photosensor amplifier (Hamamatsu C6386), and an ICCD camera were used to measure the luminance and IR emission. To produce the boundary image sticking, the entire region of the 42 in. panel was changed to a full-white background image immediately after displaying a square-type image (region A) at peak luminance for approximately 500 h. Using the automatic power control system of the PDP, approximately 1500 sustained pulses were alternately applied to the X and Y electrodes during one TV field (=16.67 ms) to display a square-type test image with a 1% display region within the entire region of the 42 in. panel. The conventional driving method with a selective reset waveform was adopted. The frequency for a sustained period was 200 kHz, and the sustained voltage was 205 V. The gas was filled to a pressure of 430 Torr. The detailed panel specifications used in this experiment are exactly the same as those listed in Table 1, except for the sealing process for the vacuum-sealing case and the working pressure for the lower pressure case.

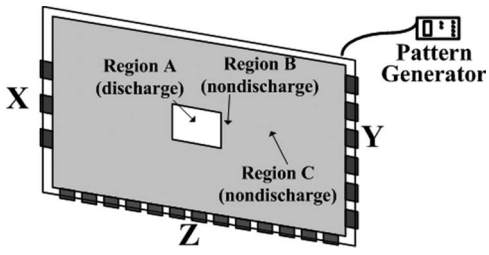

Fig. 1. Schematic diagram of the experimental setup used in this research.

Table 1. Specifications of the 42 in. ac PDP Used in This Study

Front Panel		Rear Panel	
ITO width	225 μm	Barrier rib width	55 μm
ITO gap	85 μm	Barrier rib height	120 μm
Bus width	50 μm	Address width	95 μm
Pixel Pitch		912 μm × 693 μm	
Gas chemistry		Ne–Xe (15%)–He (35%)	
Barrier rib type		Closed rib	

3. Boundary Image Sticking Phenomenon in an ac Plasma Display Panel and Its Mechanism

Figure 2(a) shows the image sticking pattern captured under the full-white background of the 42 in. panel. Figure 2(b) shows the imaging pattern that illustrates the luminance difference among regions A, B, and C in Fig. 2(a), which were measured by use of an imaging colorimeter camera with RGB filters. Region A indicates the image sticking cells, region B indicates the boundary image sticking cells, and region C indicates the normally working cells. In the absence of any image sticking phenomenon, the luminance in Fig. 2(b) would be almost the same among the three regions. However, as shown in Fig. 2(b), the three regions exhibit a different luminance with the full-white background because of the image sticking induced by the iterant strong sustained discharge in region A. Even though no iterant strong sustained discharge was produced in region B, the image sticking phenomenon was still observed, and, since the region formed a circular shape, it is hereinafter referred to as halo-type boundary image sticking.

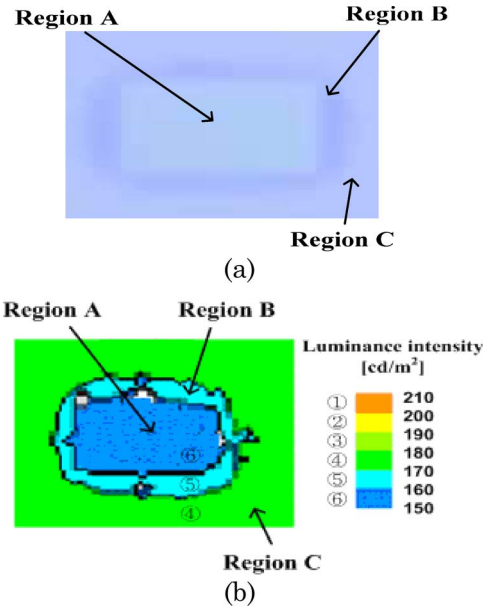

Fig. 2. (Color online) (a) Image sticking pattern captured under full-white background of a 42 in. panel and (b) imaging pattern showing luminance difference among regions A, B, and C in (a) measured with an imaging colorimeter: region A, image sticking cells; region B, halo-type boundary image sticking cells; region C, normal working cells.

Figure 3(a) shows the changes in the IR (828 nm) emission intensity measured from regions A, B, and C during the sustained period under the full-white background. Figure 3(b) shows the IR emission profiles measured at a peak time of IR emission in Fig. 3(a) by using the gate mode of the ICCD. As shown in Figs. 3(a) and 3(b), the IR emission peak for region B was observed to be shifted to the left and intensified compared with that for region C, indicating that the strong sustained discharge was efficiently initiated at a lower starting discharge voltage and intensified during the sustained period, thereby producing the halo-type boundary image sticking. To investigate the reason for producing the halo-type boundary image sticking, the SEM images of the MgO surfaces after an iterant sustained discharge (500 h) were measured in regions A, B, and C. Figure 4 shows the changes in the plane and cross-sectional SEM images of the MgO surfaces captured from regions A, B, and C. Although the cells in region B were nondischarge cells, the morphology of the MgO surface in region B was observed to be changed, as shown in Fig. 4(a), and the redeposited MgO layer above the original MgO layer was also observed, as shown in Fig. 4(b).

Theoretically, the morphology of the MgO surface in the cells should not change if the strong sustained discharge is not produced repeatedly in the cells. Nonetheless, a change was observed in the morphology of the MgO surface of the nondischarge cells (region B) due to the redeposition of the Mg species sputtered by the iterant strong sustained discharge in discharge region A adjacent to nondischarge region B, as shown in Figs. 4(a) and 4(b). Although the Mg species were predominantly sputtered and redeposited in discharge region A, there was also a slight redeposition in nondischarge region B adjacent to discharge region A. As a result, the cross-sectional SEM analysis in Fig. 4(b) confirmed that the halo-type boundary image sticking phenomenon was predominantly due to the redeposition of Mg species on the MgO layer in the nondischarge region adjacent to the discharge region.

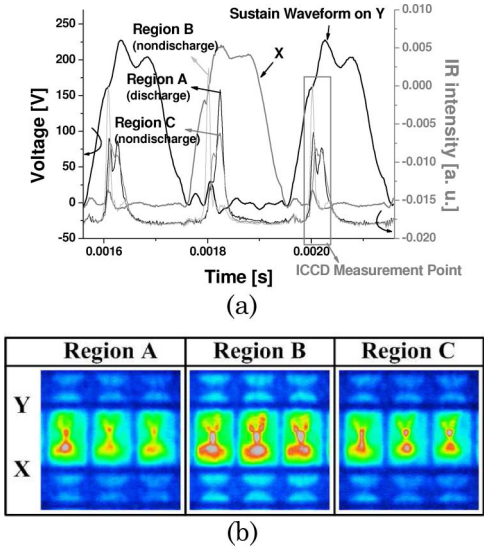

Fig. 3. (Color online) (a) IR (828 nm) emission intensities measured from regions A, B, and C during a sustained period under full-white background after 500 h sustained discharge and (b) IR emission profiles measured at the peak of IR emission in (a) by use of the gate mode of the ICCD.

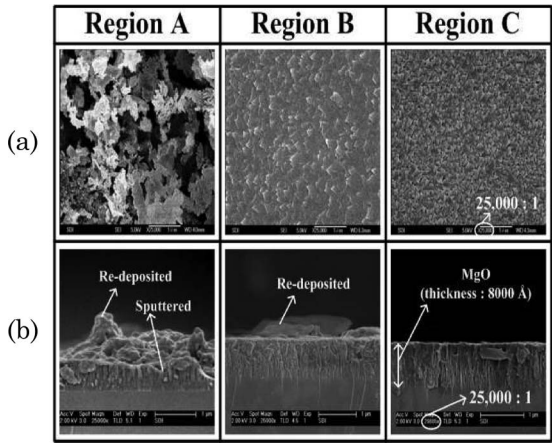

Fig. 4. Comparison of the (a) plane SEM image of the MgO surface and (b) the cross-sectional SEM image of the MgO layer for regions A, B, and C after 500 h sustained discharge.

4. Solutions to Remove a Boundary Image Sticking in an ac Plasma Display Panel

To remove the boundary image sticking, three solutions are proposed. The first is to completely recover the boundary image sticking cells by means of the full-white aging process when boundary image sticking has already been produced. The second solution is to prohibit the inherent production of boundary image sticking by sealing the PDP panel under vacuum. The third solution is to prohibit the inherent production of boundary image sticking by lowering the gas pressure of the PDP panel.

A. Recovery Using a Full-White Aging Discharge

Before full-white aging discharge, as shown in Figs. 3 and 4, the IR emission and morphology of the MgO surface in region B were changed compared with that for region C. As mentioned before, this phenomenon in region B seemed to occur because of the redeposition of Mg transported from region A, where the MgO surface was sputtered during the iterant strong sustained discharge. Table 2 compares the image sticking production condition and full-white aging

Table 2. Comparison of Image-Sticking Production Conditions and Full-White Aging Discharge Conditions

Condition	Displayed Area	Pulse Number per 1 TV Field	Total Discharge Time (h)
Image sticking production	5 cm × 6 cm in 42 in.	1520	500
Full-white aging	Entire region in 42 in.	300	100

discharge condition. To eliminate the difference of the MgO surface between regions B and C, the 42 in. panel with boundary image sticking was discharged under the 100 h full-white aging discharge condition listed in Table 2 [7]. Here, the 100 h full-white aging time for recovery was chosen depending on the severity of the boundary image sticking as determined by the strong sustained discharge time. We then checked the removal of the boundary image sticking, and the entire region of the test panel was changed to the full-white background image immediately after the full-white aging discharge.

Figure 5(a) shows the changes in the IR (828 nm) emission intensity measured from regions A, B, and C during the sustained period under the full-white background. Figure 5(b) shows the IR emission profiles measured at a peak time of IR emission in Fig. 5(a) by using the gate mode of the ICCD. Unlike the IR emission in Fig. 3, the IR emission data in Fig. 5 illustrates that, after the full-white aging discharge, the ignition time and intensity of the IR (828 nm) emission waveforms show no difference between regions B and C, confirming that the full-white aging discharge contributed to the recovery of IR emission characteristics of the boundary image sticking cells. As a result, the luminance in regions B and C under full-white background was also observed to be almost the same, thanks to the recovery of IR emission in the boundary image sticking cells (luminance in region A, approximately 155 cd/m^2; region B, approximately 165 cd/m^2; region C, approximately 165 cd/m^2).

Figure 6 shows the change in the plane SEM image of the MgO surfaces for regions A, B, and C after full-white aging discharge. During the full-white aging

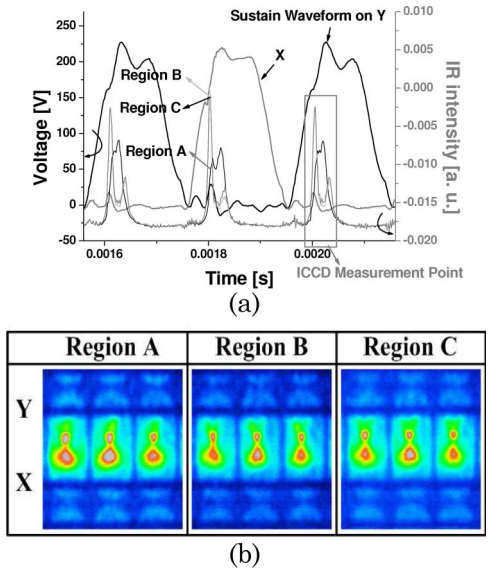

Fig. 5. (Color online) (a) IR (828 nm) emission intensities measured from regions A, B, and C during the sustained period under a full-white background after full-white aging discharge in a 42 in. test panel with boundary image sticking and (b) IR emission profiles measured at the peak of IR emission in (a) by use of the gate mode of the ICCD.

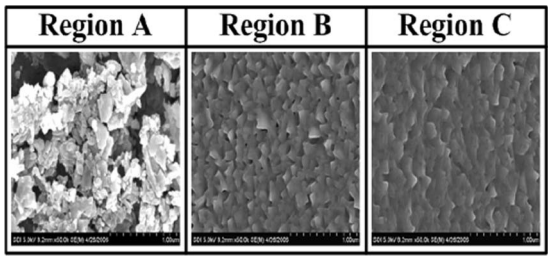

Fig. 6. Plane SEM images of MgO surfaces for regions A, B, and C after full-white aging discharge.

discharge, the ions bombarded the MgO surfaces in all three regions. As shown in Fig. 6, the resultant MgO surface in region A, i.e., the image sticking region, became rougher with a larger grain size. However, in region B (the boundary image sticking region), the MgO surface revealed a smaller grain size after the full-white discharge with a similar surface morphology to the MgO layer in region C. In regions B and C, the sustained discharges were simultaneously produced for 100 h under the full-white aging discharge condition, yet ion bombardment was less intense than that under the 500 h sustained discharge for displaying the test image with a 1% display area. Thus, the surface morphologies of the MgO layers in regions B and C were similar as a result of the full-white aging discharge, as shown in Fig. 6. As a result, the SEM images in Fig. 6 confirm that the simultaneous ion bombardment under full-white aging discharge caused the MgO surfaces in regions B and C to equalize, especially the redeposited MgO surface in region B. Therefore, the 100 h full-white aging discharge contributed to the recovery of the boundary image sticking.

B. Prevention of Boundary Image Sticking Using a Vacuum Sealing Method

Based on the idea that the impurity level in a PDP is closely related to the boundary image sticking phenomenon, the effects of the vacuum sealing process on the production of boundary image sticking were examined [8,9]. In the vacuum sealing process, the base vacuum level was enhanced from 10^{-2} to 10^{-5} Torr [14–17]. In the 42 in. test panel prepared by the vacuum sealing process instead of the conventional atmospheric pressure sealing process, the square-type image (region A) in Fig. 1 was displayed for 500 h.

Figure 7(a) shows the changes in the IR (828 nm) emission intensity measured from regions A, B, and C during the sustained period under a full-white background after displaying a square-type image for 500 h in the 42 in. test panel prepared by using the vacuum sealing process. Figure 7(b) shows the IR emission profiles measured at the peak of IR emission in Fig. 7(a) by using a gate mode of the ICCD. For the vacuum sealing case, the ignition time and intensity of the IR emission were observed to have no difference between regions B and C [8], as shown in Figs. 7(a) and 7(b). As a result, the luminance in

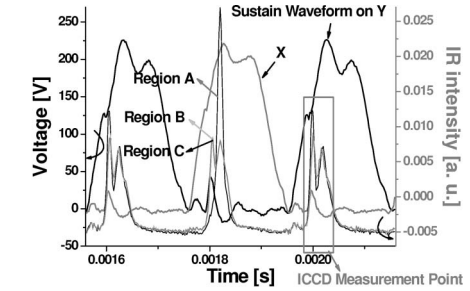

(a)

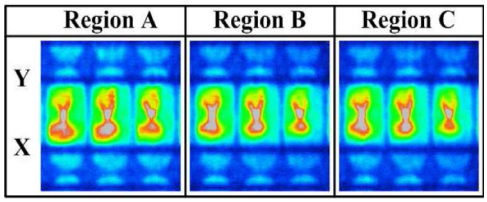

(b)

Fig. 7. (Color online) (a) IR (828 nm) emission intensities measured from regions A, B, and C during the sustained period under a full-white background after 500 h sustained discharge in a 42 in. test panel prepared by use of vacuum sealing and (b) IR emission profiles measured at the peak of IR emission in (a) by use of the gate mode of the ICCD.

regions B and C under full-white background was also observed to be almost the same (luminance in region A, approximately 165 cd/m^2; region B, approximately 180 cd/m^2; region C, approximately 180 cd/m^2).

Figure 8 shows the plane SEM images of MgO surfaces captured from regions A, B, and C in the test panel prepared by the vacuum sealing process. For the vacuum sealing case, the MgO surface morphology in region B was observed to be almost similar to that in region C after the 500 h sustained discharge. This result means that the vacuum sealing method contributes to completely prohibiting the production of the boundary image sticking itself. Consequently, these results demonstrate that it was the low O_2 impurity level of the test panel prepared by using the vacuum sealing process that essentially enabled the inherent prevention of boundary image sticking in the adjacent cells, even when a strong sustained discharge was continuously produced in the discharge cells [8].

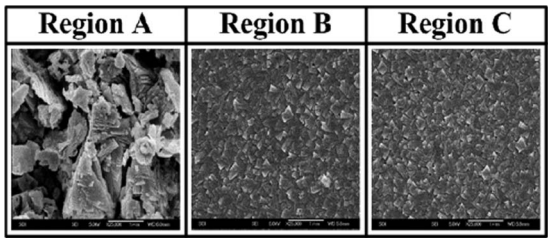

Fig. 8. Plane SEM images of MgO surfaces for regions A, B, and C after 500 h sustained discharge in a test panel prepared by use of vacuum sealing.

C. Prevention of Boundary Image Sticking Using a Lower Gas Pressure

The effects of the low gas pressure (100 Torr) on the production of boundary image sticking were examined [10,11]. Figure 9(a) shows the changes in the IR (828 nm) emission intensities measured from regions A, B, and C during the sustained period under full-white background after the 500 h sustained discharge in the 42 in. test panel prepared by using a low gas pressure of 100 Torr. Figure 9(b) shows the IR emission profiles measured at a peak time of IR emission in Fig. 9(a) by using a gate mode of the ICCD. In a low gas pressure (=100 Torr) condition, the ignition time and intensity of the IR emission were also observed to have no difference between regions B and C, similar to the vacuum sealing method, as shown in Figs. 9(a) and 9(b). As a result, the luminance in regions B and C under full-white background was also observed to be almost the same (region A, approximately 20 cd/m^2; region B, approximately 65 cd/m^2; region C, approximately 65 cd/m^2).

Figure 10 shows the plane SEM images of MgO surfaces captured from regions A, B, and C in the test panel with a low pressure of 100 Torr. For the low pressure case, the MgO surface morphology in region B was observed to be almost similar to that in region C after the 500 h sustained discharge, implying that the low gas pressure of 100 Torr also contributes to completely prohibiting the production of boundary image sticking. It is possible that the low process condition causes the redeposition of Mg particles transported from the discharge cells to be suppressed in the boundary image sticking cells.

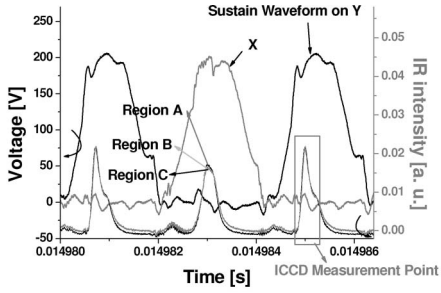

(a)

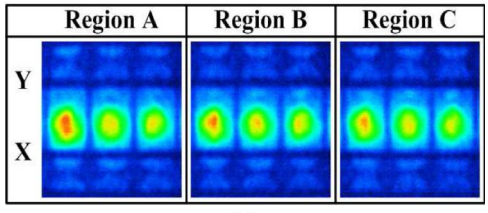

(b)

Fig. 9. (Color online) IR (828 nm) emission intensities measured from regions A, B, and C during a sustained period under full-white background after 500 h sustained discharge in a 42 in. test panel prepared by use of low (100 Torr) gas pressure and (b) IR emission profiles measured at the peak of IR emission in (a) by use of the gate mode of the ICCD.

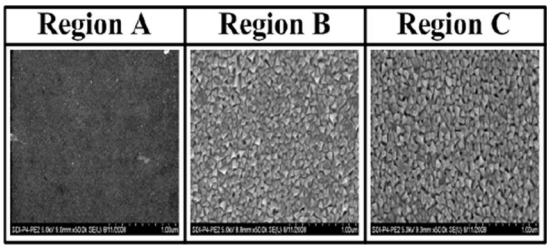

Fig. 10. Plane SEM images of MgO surfaces for regions A, B, and C after 500 h sustained discharge in a 42 in.. test panel prepared by use of low (100 Torr) gas pressure.

5. Conclusion

When displaying the square-type image with peak luminance for a long time in a plasma display panel TV, the image sticking appears even in the nondischarge cells adjacent to the discharge cells, which is called boundary image sticking. The boundary image sticking phenomenon is predominantly due to the redeposition of the Mg species on the MgO layer in the nondischarge region adjacent to the discharge region. We have proposed three methods than can be used to remove boundary image sticking. The first is to completely recover the boundary image sticking cells by means of full white-aging process. The second is to prohibit inherently the production of boundary image sticking by sealing the PDP panel under vacuum. The final method is to prohibit the inherent production of boundary image sticking at a lower gas pressure.

This research was supported in part by the Information Technology Research and Development program of the Ministry of Knowledge Economy (MKE), Korea Evaluation Institute of Industrial Technology (KEIT) and in part by the Brain Korea 21 project (BK21).

References

1. H.-S. Tae, C.-S. Park, B.-G. Cho, J.-W. Han, B. J. Shin, S.-I. Chien, and D. H. Lee, "Driving waveform for reducing temporal dark image sticking in AC plasma display panel based on perceived luminance," IEEE Trans. Plasma Sci. **34**, 996–1003 (2006).
2. H.-S. Tae, J.-W. Han, S.-H. Jang, B.-N. Kim, B. J. Shin, B.-G. Cho, and S.-I. Chien, "Experimental observation of image sticking phenomenon in AC plasma display panel," IEEE Trans. Plasma Sci. **32**, 2189–2196 (2004).
3. J.-W. Han, H.-S. Tae, B. J. Shin, S.-I. Chien, and D. H. Lee, "Experimental observation of temperature-dependent characteristics for temporal dark boundary image sticking in 42 in. AC-plasma display panel," IEEE Trans. Plasma Sci. **34**, 324–330 (2006).
4. J. H. Kim, C.-S. Park, B.-S. Kim, K.-H. Park, and H.-S. Tae, "Comparison of temporal dark image sticking produced by face-to-face and coplanar sustain electrode structures," J. Inf. Disp. **8**, 29–33 (2007).
5. C.-S. Park, B.-G. Cho, and H.-S. Tae, "Reduction of the temporal bright-image sticking in AC-PDP modules using the vacuum sealing method," J. Inf. Disp. **9**, 39–44 (2008).
6. C.-S. Park, H.-S. Tae, Y.-K. Kwon, and E. G. Heo, "Experimental observation of halo-type boundary image sticking in AC plasma display panel," IEEE Trans. Electron. Devices **54**, 1315–1320 (2007).
7. C.-S. Park, H.-S. Tae, Y.-K. Kwon, and E. G. Heo, "Recovery of boundary image sticking using aging discharge in AC plasma display panel," IEEE Trans. Plasma Sci. **35**, 1511–1517 (2007).
8. C.-S. Park, H.-S. Tae, Y.-K. Kwon, E. G. Heo, and B.-H. Lee, "Prevention of boundary image sticking in AC plasma display panel using vacuum sealing process," IEEE Trans. Electron. Devices **55**, 1345–1351 (2008).
9. C.-S. Park and H.-S. Tae, "A study on temporal dark image sticking in AC-PDP using vacuum-sealing method," IEICE Trans. Electron. **E92-C**, 161–165 (2009).
10. C.-S. Park, S.-K. Jang, J.-H. Kim, H.-S. Tae, E.-Y. Jung, J.-C. Ahn, and E. G. Heo, "Influence of temporal and permanent image sticking characteristics under variable panel working gas pressure in 42 in. AC-PDPs," in *Proceedings of the International Meetings on Information Display/International Display Manufacturing Conference* (Korean Information Display Society, 2008), pp. 1617–1620.
11. T. Kosaka, K. Sakita, and K. Betsui, "Firing voltage fluctuation phenomenon caused by gas density nonuniformity in PDPs," in *Proceedings of the International Display Workshops* (Institute of Image Information and Television Engineers, 2005), pp. 1469–1472.
12. M. J. Jeon, M. S. Chung, S. C. Lee, K. S. Lee, J. S. Kim, and B. K. Kang, "Influence of wall charge on image sticking phenomena in AC plasma display panels," Displays **30**, 39–43 (2009).
13. L. C. Pitchford, J. Wang, D. Piscitelli, and J.-P. Boeuf, "Ion and neutral energy distribution to the MgO surface and sputtering rates in plasma display panel cells," IEEE Trans. Plasma Sci. **34**, 351–359 (2006).
14. S. J. Kwon and C.-K. Jang, "Effects of base vacuum level on discharge characteristics in vacuum in-line sealing process for high efficient PDP," J. Inf. Disp. **5**, 7–11 (2004).
15. D.-J. Lee, S.-I. Moon, Y.-H. Lee, and B.-K. Ju, "Vacuum in-line packing technology of AC-PDP using direct-joint method," in *Proceedings of the International Meeting on Information Display* (Korean Information Display Society, 2001), pp. 495–498.
16. K. Uchida, G. Uchida, T. kurauchi, T. Terasawa, H. Kajiyama, and T. Shinoda, "Evaluation of discharge voltage in AC-PDP manufactured under the vacuum condition after MgO deposition," in *Proceedings of the International Display Workshops* (Institute of Image Information and Television Engineers, 2006), pp. 347–350.
17. C.-S. Park, H.-S. Tae, Y.-K. Kwon, and E. G. Heo, "Discharge characteristics of AC plasma display panel prepared using vacuum sealing method," IEEE Trans. Plasma Sci. **36**, 1925–1929 (2008).